Electronic Supplementary Information

Plasmon Enhanced Upconversion Luminescence of NaYF$_4$:Yb, Er@SiO$_2$@Ag Core-shell Nanocomposites for Cell Imaging

Peiyan Yuan,[1,2] Yih Hong Lee,[1] Muthu Kumara Gnanasammandhan,[3] Zhenping Guan,[1] Yong Zhang,[3*] Qing-Hua Xu[1,2*]

[1]Department of Chemistry, National University of Singapore, Singapore 117543

[2]NUSNNI-Nanocore, National University of Singapore, Singapore 117576

[3] Department of Bioengineering, National University of Singapore, Singapore 117576

Email: chmxqh@nus.edu.sg (QHX); biezy@nus.edu.sg (YZ)

1. TEM images, distribution histograms and UV-Vis exctinction spectra of various NaYF$_4$:Yb, Er@SiO$_2$@Ag core-shell nanocomposites
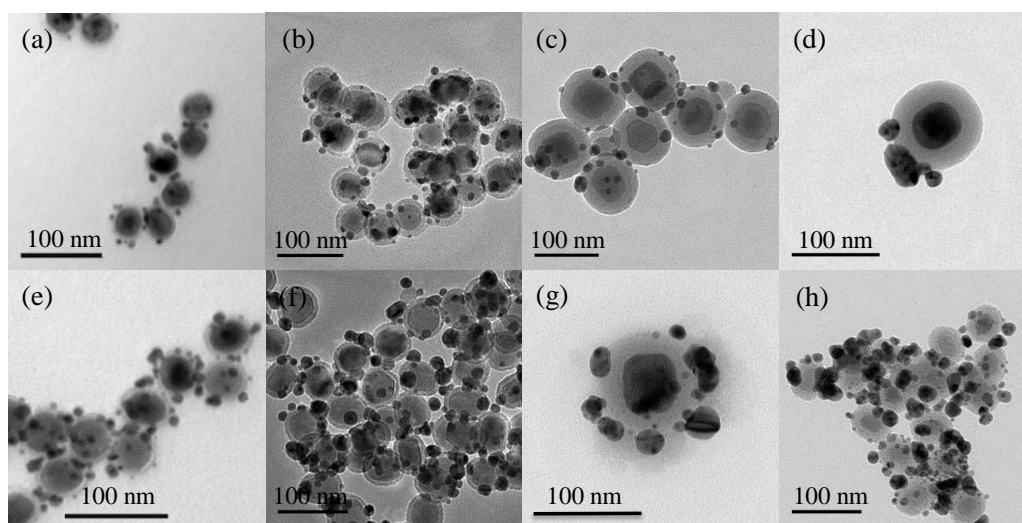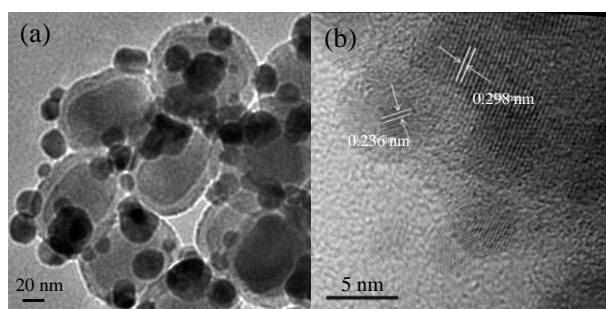

Figure S1. TEM images of NaYF$_4$:Yb,Er@SiO$_2$(3nm)@Ag(15nm) (a), NaYF$_4$:Yb,Er@SiO$_2$(10nm)@Ag(15nm) (b), NaYF$_4$:Yb,Er@SiO$_2$ (20nm)@Ag(15nm) (c), NaYF$_4$:Yb,Er@SiO$_2$(30 nm)@Ag(15nm) (d), NaYF$_4$:Yb,Er@SiO$_2$(3nm)@Ag(30nm) (e), NaYF$_4$:Yb,Er@SiO$_2$(10nm)@Ag(30nm) (f), NaYF$_4$:Yb,Er@SiO$_2$(20nm)@Ag (30nm) (g), and NaYF$_4$:Yb,Er@SiO$_2$(20nm)@Ag(30nm) (h) nanocomposites.
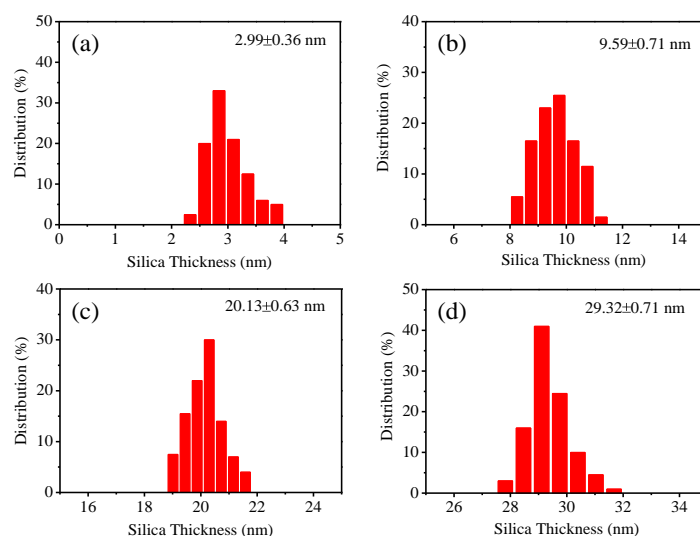
Figure S2. Size-distributions of the different silica thickness based on the size analysis of over 200 particles from TEM images: (a) NaYF$_4$:Yb,Er@SiO$_2$ (~3 nm); (b) NaYF$_4$:Yb,Er @SiO$_2$ (~10 nm); (c) NaYF$_4$:Yb,Er@SiO$_2$ (~20 nm); (d) NaYF$_4$:Yb,Er@SiO$_2$ (~30 nm).
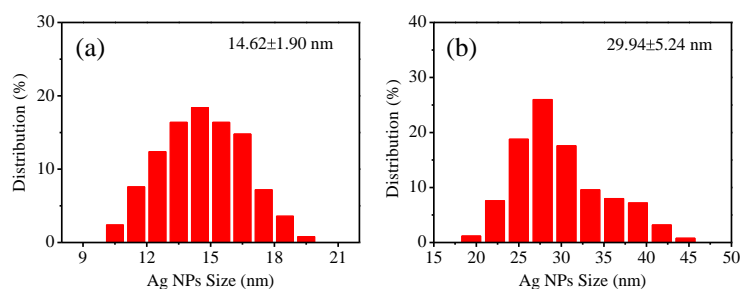
Figure S3. Size-distributions of the Ag NPs on the surface of NaYF$_4$:Yb,Er@SiO$_2$ nanoparticles based on the size analysis of over 200 particles from TEM images: (a) NaYF$_4$:Yb,Er@SiO$_2$@Ag(~15 nm); (b) NaYF$_4$:Yb,Er @SiO$_2$@Ag(~30 nm).

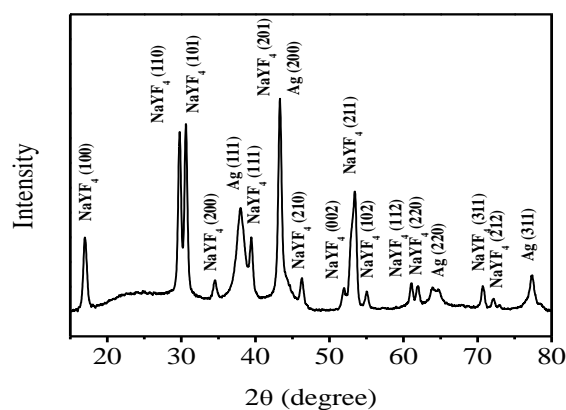**Figure S4.** (a) High-magnification and (b) high-resolution TEM images of NaYF4:Yb,Er@SiO$_2$(10nm)@Ag (30nm) nanocomposites.
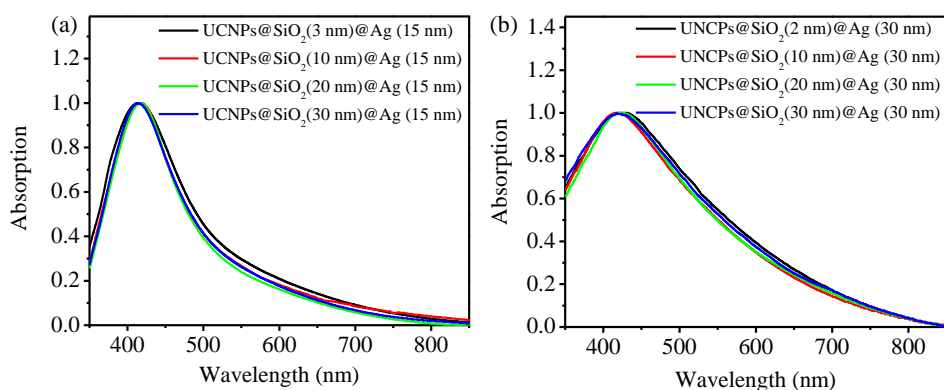
Figure S5. The UV-Vis absorption spectra of NaYF$_4$:Yb,Er@SiO$_2$@Ag(15 nm) (a) and NaYF$_4$:Yb,Er@SiO$_2$@Ag(30 nm) (B) with different SiO$_2$ spacer thickness.

2. XRD analysis of NaYF$_4$:Yb,Er@SiO$_2$@Ag nanocomposites.

Figure S6. XRD result of NaYF$_4$:Yb,Er@SiO$_2$(10 nm)@Ag(30 nm) nanocomposites. The peak positions and intensities of the nanocomposites agree well with the calculated values for NaYF$_4$:Yb,Er (JCPDS.No.28-1192) and Ag (JCPDS.No.04-0783).

3. TEM images of NaYF$_4$:Yb, Er@SiO$_2$@Ag core-shell nanocomposites before and after dissolving the Ag NPs.
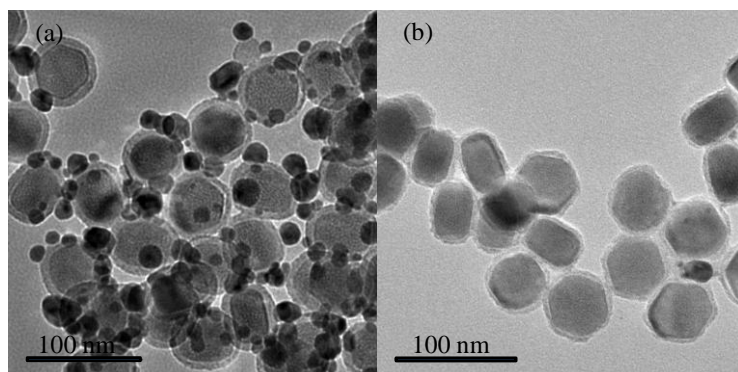
Figure S7. TEM images of NaYF$_4$:Yb, Er@SiO$_2$@Ag core-shell nanocomposites before and after dissolving the Ag NPs.

4. Distance and particle radius dependent enhancement mechanisms

Based on the theory developed by Bharadwaj and Novotny (reference 29: *Opt. Express*, 2007, **15**, 14266-14274), the radiative decay rate (γ_r) and energy transfer rate (γ_{abs}) of a chromophore in proximity of metal surface depends on the separation distance between them. The separation distance dependence can be quantitatively described by

$$\frac{\gamma_r}{\gamma_r^o} = \left| 1 + 2\frac{a^3}{(a+z)^3}\frac{\varepsilon(\omega_2)-1}{\varepsilon(\omega_2)+2} \right|^2$$

eq.1

$$\frac{\gamma_{abs}}{\gamma_r^o} = \frac{3}{16} \operatorname{Im}\frac{\varepsilon(\omega_2)-1}{\varepsilon(\omega_2)+1}\frac{1}{k_2^3 z^3}\frac{(p_x^2 + p_y^2 + 2p_z^2)}{|\mathbf{p}|^2}$$

eq.2,

where a is the particle radius and z is the separation distance. At direct contact between m chromophores and surface of metal nanoparticles, energy transfer rate (γ_{abs}) is very large (inversely proportional to z^3 according to eq 2). The non-radiative energy transfer is the dominant excited state deactivation channel, which will cause decreased emission efficiency. Energy transfer rate (γ_{abs}) decreases rapidly as a function of z^{-3}, as the separation of separation distance z increases. However, radiative decay rate (γ_r) only decreases mildly, for distance z smaller or comparable to the particle radius. The

energy transfer rate will decrease more rapidly than the radiative decay rate as the separation distance increases. The quantum yield, $QY=\gamma_r /(\gamma_r +\gamma_{abs})$, will increases to achieve emission enhancement as the separation distance increases. At very large separation distances, the radiative decay rate will not be affected and energy transfer process does not occur. The luminescence efficiency will not be affected by the presence of metal nanoparticles for very large separation distances. Consequently, the optimum enhance occur at some intermediate separation distance (see Figure 2 in ref. 29).

The particle size dependent enhancement could also be understood using the above formulas. According to eq.1, the radiative decay rate (γ_r) decreases less rapidly for particle with a larger radius (a) as the separation distance z increases. This explains our observed relative milder separation distance dependent enhancement for 30 nm Ag NPs in comparison with the 15 nm NPs.

5. The effect of DNA modification to the emission spectra of NaYF$_4$:Yb,Er@SiO$_2$(10nm)@Ag(15nm) nanocomposites.
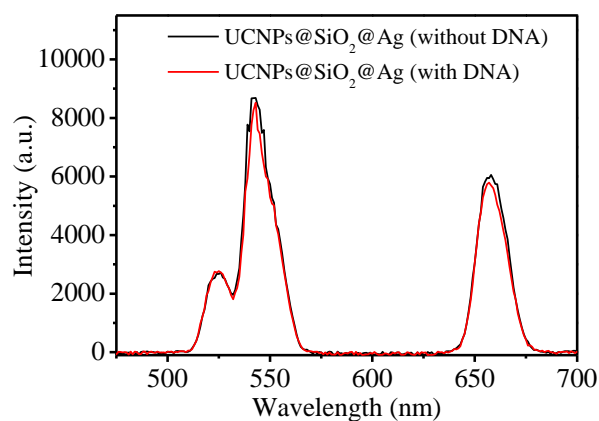
Figure S8. Emission spectra of NaYF$_4$:Yb,Er@SiO$_2$(10nm)@Ag(15nm) nanocomposites with and without modification with DNA.

6. Bright field cell imaging experiment.
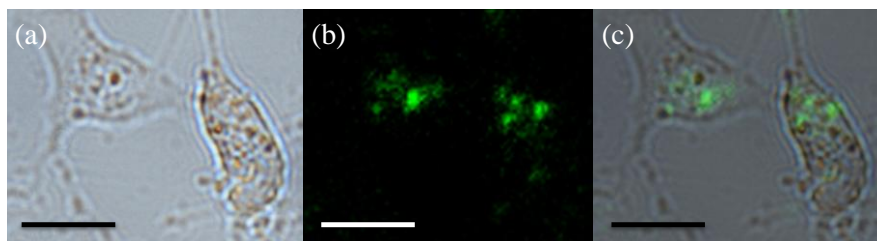
Figure S9. (a) Bright field imaging of live B16F0 cells after incubation with DNA-modified NaYF$_4$:Yb,Er@SiO$_2$(10 nm)@Ag(15 nm) nanocomposites, (b) Fluorescence of NaYF$_4$:Yb,Er@SiO$_2$(10 nm)@Ag(15 nm) nanocomposites (50 µg/mL) (green) and The merged images are shown in (c). (Scale bar:20 µm)

7. Cell viability before and after cell imaging experiments.

We have measured the cell viability before and after the cell imaging experiments (The laser power: 500 mW; the objective: 40x; the nanoparticles concentration: 50 µg/mL). The result showed that the cells remained alive after the imaging experiments and the excitation caused negligible photo-damage to the cells.
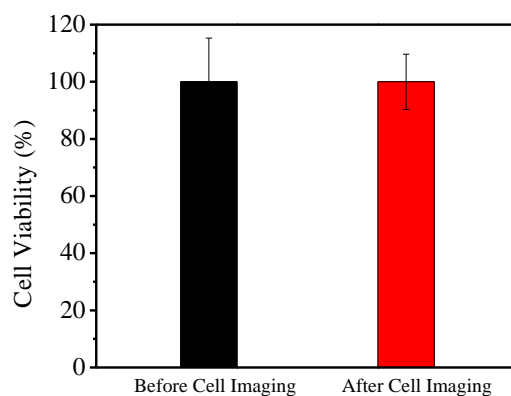

Figure S10. Cell viability before and cell imaging using upconversion nanocrysrtals.

8. The dynamic light scattering (DLS) analysis of NaYF$_4$:Yb,Er@SiO@Ag nanocomposites.
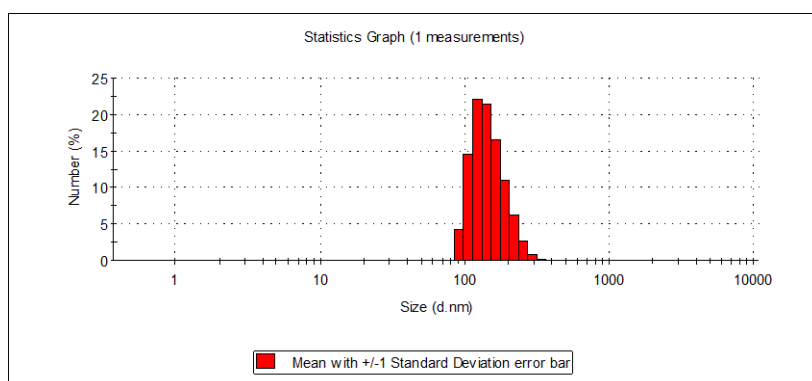
Figure S11. DLS size distribution of NaYF$_4$:Yb,Er@SiO$_2$(10 nm)@Ag(15 nm) nanocomposites in water.

9. Stability of luminescence intensity and size changes of the DNA modified nanocomposites in the cell culture
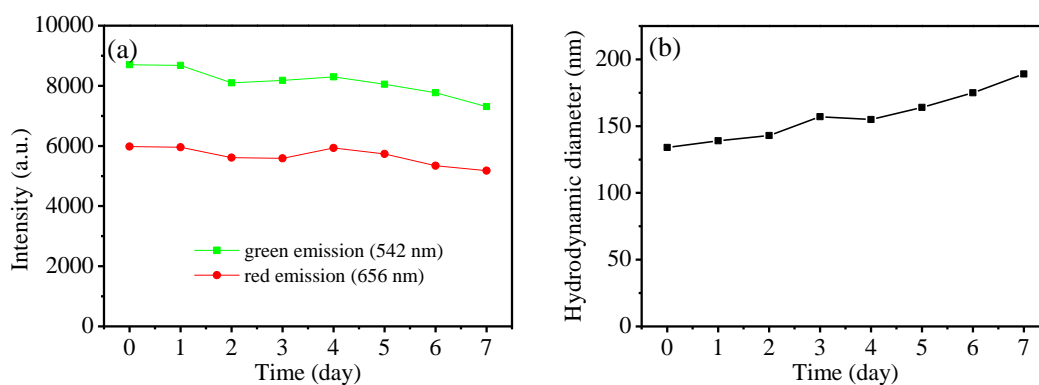
Figure S12. Stability of luminescence intensity (a) and size changes (b) of the DNA modified NaYF$_4$:Yb,Er@SiO$_2$(10 nm)@Ag(15 nm) nanocomposites in the cell culture solution for 7 days. The results confirm that these DNA modified nanocomposites are quite stable.